Progress In Electromagnetics Research, PIER 70, 37–52, 2007

CHARACTERISTICS OF ELECTROMAGNETIC WAVE PROPAGATION IN BIAXIALLY ANISOTROPIC LEFT-HANDED MATERIALS

W. Ding, L. Chen, and C.-H. Liang

National Key Lab of Antenna and Microwave Technology
Xidian University
Xi'an 710071, China

Abstract—This paper investigates the characteristics of electromagnetic wave propagation in biaxially anisotropic left-handed materials (BA-LHMs) theoretically and numerically. We discuss under what conditions the anomalous refraction or reflection will occur at the interface when a plane wave passes from one isotropic right-handed material into another BA-LHM. Meanwhile the refraction angle of the wave vector and that of the Poynting power are presented when the anomalous refraction takes place. According to the theoretical analysis, several sets of constitutive parameters of BA-LHMs are considered. Then the anomalous refraction or reflection of the continuous-wave (CW) Gaussian Beam passing from free space into BA-LHMs are simulated by the finite difference time domain (FDTD) method based on the Drude dispersive models. The simulated results are in agreement with theoretical results, which validates the theoretical analysis.

1. INTRODUCTION

In 1968, Veselago [1] investigated theoretically the propagation of electromagnetic wave in materials with simultaneously negative permittivity ε and negative permeability μ or left-handed materials (LHMs). He predicted that the wave vector $\boldsymbol{k}$ would form a left-handed triad with the electric field $\boldsymbol{E}$ and the magnetic field $\boldsymbol{H}$ inside a LHM and that some interesting electromagnetic properties such as negative refraction index, reversed Doppler effect and reversed Cerenkov radiation would be obtained. But his idea was forgotten because LHMs were not available at that time. It was not until 1998 when Pendry et al. experimentally demonstrated negative ε in low frequency plasma using thin wires [2] and negative μ using split

ring resonators (SRRs) that LHMs could be finally realized [3]. Soon afterwards, following Pendry's discovery, Smith et al. demonstrated for the first time the existence of LHMs by combining a two-dimensional (2D) array of SRRs interspersed with a 2D array of wires [4] and also later experimentally demonstrated the negative refraction index of LHMs [5]. From then on, the researches on LHMs have gained significant interest and become more and more comprehensive and extensive.

However, Veselago's original paper and most of the recent theoretical works discussed mainly the characteristics of electromagnetic wave propagation in isotropic LHMs, in which ε and μ are both negative scalars. But up to now, the LHMs that have been prepared successfully in experiments are actually anisotropic in nature, and it may be very difficult to prepare an isotropic LHM [1, 4, 5]. It is currently well accepted that a better model is to consider anisotropic constitutive parameters, which can be diagonalized in the coordinate system collinear with the principal axes of the metamaterial. So the researches on characteristics of electromagnetic wave propagation in anisotropic LHMs become more and more important and practical. As far as the authors know, most researches focus mainly on uniaxially anisotropic LHMs (UA-LHMs) [6–10], in which ε and μ tensors are simultaneously diagonalizable and each tensor includes two principal constants in the directions parallel and perpendicular to the principal axis. In this paper, we present an investigation on the characteristics of electromagnetic wave propagation in biaxially anisotropic LHMs (BA-LHMs) theoretically and numerically. Each of diagonalizable ε and μ tensors in BA-LHMs includes three different principal constants. So BA-LHMs can be reduced to UA-LHMs if the two components in the directions perpendicular to the principal axis are equal and they can be also reduced to isotropic LHMs if the three components are equal, which makes BA-LHMs more general and practical than UA-LHMs.

This paper mainly includes three sections: In Section 2, taking a TE polarized plane wave (electric field along $+z$ and $k_z = 0$) as an example, we deduce the dispersion relation for the plane wave in BA-LHMs. In Section 3, we discuss under what conditions the anomalous refraction or reflection will occur at the interface when the TE polarized plane wave passes from one isotropic right-handed material (RHM) into another BA-LHM and present the refraction angle of the wave vector and that of the Poynting power when the anomalous refraction takes place. In Section 4, the finite difference time domain (FDTD) method based on the Drude dispersive models [11, 12] is employed to simulate the anomalous refraction or reflection of the continuous-wave (CW) Gaussian Beam passing from free space into BA-LHMs with several

sets of constitutive parameters. The results validate the theoretical analysis.

2. DISPERSION RELATION IN BIAXIALLY ANISOTROPIC LEFT-HANDED MATERIALS

For anisotropic materials, one or both of the permittivity and permeability are second-rank tensors. In the following we assume that both the permittivity and permeability are biaxially anisotropic with ε and μ tensors that are simultaneously diagonalizable,

$$\overline{\overline{\varepsilon}} = \varepsilon_0 \overline{\overline{\varepsilon}}_r = \varepsilon_0 \mathrm{diag}\left[\varepsilon_{rx}, \varepsilon_{ry}, \varepsilon_{rz}\right] = \mathrm{diag}\left[\varepsilon_x, \varepsilon_y, \varepsilon_z\right] \tag{1a}$$

$$\overline{\overline{\mu}} = \mu_0 \overline{\overline{\mu}}_r = \mu_0 \mathrm{diag}\left[\mu_{rx}, \mu_{ry}, \mu_{rz}\right] = \mathrm{diag}\left[\mu_x, \mu_y, \mu_z\right] \tag{1b}$$

where not all of the principal components have the same sign for BA-LHMs. So metamaterials composed of an arrangement of rings (either split rings, Ω-rings [13], S-rings [14, 15], symmetrical ring [16], or others) and rods can be readily constructed that closely approximate these ε and μ tensors, with elements of either algebraic sign [17].

From Maxwell's equations, all plane waves in the medium can be split into TE and TM waves, and they can be considered separately. Without losing any generality, this paper only discusses the characteristics of TE plane waves propagation in BA-LHMs. As to TM plane waves, the characteristics can be obtained through duality, by interchanging corresponding permittivity and permeability components in Eq. (1). Now taking a TE plane wave (electric field polarized in the $+z$ direction and $k_z = 0$) as an example, the principal axis of BA-LHMs is taken as the y axis and the wave vector $\boldsymbol{k}$ is assumed in the xoy plane, namely $\boldsymbol{k} = \boldsymbol{e}_x k_x + \boldsymbol{e}_y k_y$, so the electric field can be written by

$$\boldsymbol{E} = E_0 \boldsymbol{e}_z \exp\left(ik_x x + ik_y y - i\omega t\right) \tag{2a}$$

From $\boldsymbol{k} \times \boldsymbol{E} = \omega \boldsymbol{B} = \omega \overline{\overline{\mu}} \cdot \boldsymbol{H}$, the magnetic field can be expressed as

$$\boldsymbol{H} = \left(\frac{k_y E_0}{\omega \mu_x} \boldsymbol{e}_x - \frac{k_x E_0}{\omega \mu_y} \boldsymbol{e}_y\right) \exp\left(ik_x x + ik_y y - i\omega t\right) \tag{2b}$$

Substitute Eqs. (1) and (2) into $\boldsymbol{k} \times \boldsymbol{H} = -\omega D = -\omega \overline{\overline{\varepsilon}} \cdot \boldsymbol{E}$, then the dispersion relation of the TE wave in BA-LHMs is

$$k_x^2/\mu_y + k_y^2/\mu_x = \omega^2 \varepsilon_z \tag{3}$$

And the time-averaged Poynting vector $\boldsymbol{S}$ and its inner product with the wave vector $\boldsymbol{k}$ can be given by

$$\boldsymbol{S} = \frac{1}{2}\mathrm{Re}\left[\boldsymbol{E} \times \boldsymbol{H}^*\right] = \frac{1}{2}\mathrm{Re}\left[\frac{k_x E_0^2}{\omega\mu_y}\boldsymbol{e}_x + \frac{k_y E_0^2}{\omega\mu_x}\boldsymbol{e}_y\right] \tag{4}$$

$$\boldsymbol{k} \cdot \boldsymbol{S} = \frac{1}{2}\mathrm{Re}\left[\varepsilon_z \omega E_0^2\right] \tag{5}$$

These expressions show that, in general, the electric field $\boldsymbol{E}$, the magnetic field $\boldsymbol{H}$ and the wave vector $\boldsymbol{k}$ cannot form a strictly left-handed triad of vectors and the direction of the power flow in each wave differs from the direction of the wave vector. One can note that the Poynting vector $\boldsymbol{S}$ and the wave vector $\boldsymbol{k}$ are not only antiparallel in the true anisotropic LHMs. The angle between them is larger than $\pi/2$ if ε_z is less than zero.

3. ANOMALOUS REFRACTION OF PLANE WAVE PROPAGATION FROM ONE ISOTROPIC RHM INTO ANOTHER BA-LHM

In this section we discuss the characteristics of the anomalous refraction of electromagnetic wave propagation from one isotropic RHM into the second BA-LHM. A schematic illustration of the system is shown in Fig. 1.

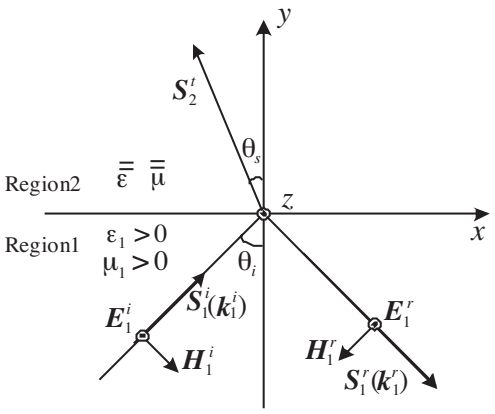

Figure 1. Illustration of anomalous refraction when a plane wave passes from one isotropic RHM into another BA-LHM.

The total space is divided into two regions. One is the isotropic RHM region with $\varepsilon_1 = \varepsilon_0\varepsilon_{r1} > 0$, $\mu_1 = \mu_0\mu_{r1} > 0$ in Region 1 ($y < 0$),

the other is the BA-LHM region with permittivity and permeability tensors denoted in Eq. (1) in Region 2 ($y > 0$). The TE polarized plane wave discussed in Section 2 passes from the left lower quadrant of Region 1 into Region 2, so the principal axis (the y axis) of the BA-LHM is normal to the interface of the two Regions. If the power flow of the refracted wave in Region 2 locates on the left side of the $+y$ axis, namely the incident and refracted waves are simultaneously on the same side of the normal, we define that the refraction is anomalous.

From Fig. 1, the wave vectors of the incident and reflected waves can be written by $\boldsymbol{k}_1^i = k_x\boldsymbol{e}_x + k_y\boldsymbol{e}_y$ and $\boldsymbol{k}_1^r = k_x\boldsymbol{e}_x - k_y\boldsymbol{e}_y$, where $(k_1^i)^2 = (k_1^r)^2 = k^2 = \omega^2\varepsilon_1\mu_1 = (k_0)^2\varepsilon_{r1}\mu_{r1}$ and $k_x > 0$, $k_y > 0$. So the electric fields of the incident and reflected waves can be obtained

$$\boldsymbol{E}_1^i = E_0\boldsymbol{e}_z \exp\left(ik_x x + ik_y y - i\omega t\right) \tag{6a}$$

$$\boldsymbol{E}_1^r = rE_0\boldsymbol{e}_z \exp\left(ik_x x - ik_y y - i\omega t\right) \tag{6b}$$

where r is the reflection coefficient. From the boundary conditions of Maxwell's equations, it can be easily shown that the tangential component of the wave vector of the refracted wave k_{2x}^t is equal to that of the incident wave, namely $k_{2x}^t = k_x > 0$. We can obtain the wave vector of the refracted wave $\boldsymbol{k}_2^t = k_x\boldsymbol{e}_x + k_{2y}^t\boldsymbol{e}_y$, so the electric field of the refracted wave can be expressed as

$$\boldsymbol{E}_2^t = tE_0\boldsymbol{e}_z \exp\left(ik_x x + ik_{2y}^t y - i\omega t\right) \tag{6c}$$

where t is the transmission coefficient and k_{2y}^t can be obtained from Eq. (3)

$$\left(k_{2y}^t\right)^2 = \omega^2\varepsilon_z\mu_x - \left(\mu_x/\mu_y\right)k_x^2 \tag{7}$$

Then the magnetic fields of the incident, reflected and refracted waves can be obtained from equation $\boldsymbol{k} \times \boldsymbol{E} = \omega\boldsymbol{B} = \omega\overline{\overline{\mu}} \cdot \boldsymbol{H}$ as follows

$$\boldsymbol{H}_1^i = \left(k_y\boldsymbol{e}_x - k_x\boldsymbol{e}_y\right)\frac{E_0}{\omega\mu_1} \exp\left(ik_x x + ik_y y - i\omega t\right) \tag{8a}$$

$$\boldsymbol{H}_1^r = -\left(k_y\boldsymbol{e}_x + k_x\boldsymbol{e}_y\right)\frac{rE_0}{\omega\mu_1} \exp\left(ik_x x - ik_y y - i\omega t\right) \tag{8b}$$

$$\boldsymbol{H}_2^t = \left(\frac{tE_0k_{2y}^t}{\omega\mu_x}\boldsymbol{e}_x - \frac{tE_0k_x}{\omega\mu_y}\boldsymbol{e}_y\right)\exp\left(ik_x x + ik_{2y}^t y - i\omega t\right) \tag{8c}$$

Because the tangential components of electromagnetic fields at the interface ($y = 0$) are equal, the reflection and transmission coefficients can be obtained

$$r = \frac{k_y\mu_x - k_{2y}^t\mu_1}{k_y\mu_x + k_{2y}^t\mu_1}; \quad t = \frac{2k_y\mu_x}{k_y\mu_x + k_{2y}^t\mu_1} \tag{9}$$

Then the time-averaged Poynting vector $\boldsymbol{S}_2^t$ in Region 2 can be obtained from Eq. (4)

$$\boldsymbol{S}_2^t = \mathrm{Re}\left[\frac{t^2 E_0^2 k_x}{2\omega\mu_y}\boldsymbol{e}_x + \frac{t^2 E_0^2 k_{2y}^t}{2\omega\mu_x}\boldsymbol{e}_y\right] \tag{10}$$

So the basic characteristics of the reflection and refraction of electromagnetic waves can be seen from Eqs. (9) and (10).

In the following section, let us discuss under what conditions the anomalous refraction will occur at the interface.

Firstly, there must be refraction taking place in Region 2, which requires the y component of the wave vector of the refracted wave k_{2y}^t must be real. If k_{2y}^t is a imaginary value, $\boldsymbol{E}_2^t$ will attenuate exponentially in the y direction from Eq. (6c) and the y component of the Poynting vector of the refracted wave will be zero, namely $\boldsymbol{e}_y \cdot \boldsymbol{S}_2^t = \mathrm{Re}\left[\left(t^2 E_0^2 k_{2y}^t\right)/(2\omega\mu_x)\right] = 0$, hence no power will be transmitted into the Region 2 and the incident wave will be totally reflected. So from Eq. (7), the refraction will occur only if the incident angle θ_i satisfies

$$(\mu_x/\mu_y)\, k^2 \sin^2\theta_i < \omega^2 \varepsilon_z \mu_x \tag{11}$$

Secondly, according to the practical physical conception, when the refraction takes place in Region 2, the power of the refracted wave must be flowing away from the interface of the two materials but never toward the interface. This requires $\boldsymbol{e}_y \cdot \boldsymbol{S}_2^t > 0$, so we can obtain the second condition as follow

$$k_{2y}^t/\mu_x > 0 \tag{12}$$

Lastly, the anomalous refraction will occur when the power flows of the incident and refracted waves are on the same side of the normal, which requires $\boldsymbol{k}_x \cdot \boldsymbol{S}_2^t = \mathrm{Re}\left[t^2 E_0^2 k_x^2/2\omega\mu_y\right] < 0$. So the last condition is

$$\mu_y < 0 \tag{13}$$

From Eqs. (11)–(13), we can obtain several sets of constitutive parameters of BA-LHMs which satisfy the conditions above at the same time.

CASE1. $\mu_y < 0$, $\mu_x < 0$, $\varepsilon_z < 0$

From Eq. (7), the components of the wave vector $\boldsymbol{k}_2^t$ in the wave-vector surface satisfy a spheroid expression $k_x^2/(\mu_y\varepsilon_z) + \left(k_{2y}^t\right)^2/(\varepsilon_z\mu_x) = \omega^2$. From Eq. (11), there exists a critical

angle for the incident wave, $\theta_c = \arcsin\sqrt{(\varepsilon_z\mu_y)/(\varepsilon_1\mu_1)} = \arcsin\sqrt{(\varepsilon_{rz}\mu_{ry})/(\varepsilon_{r1}\mu_{r1})}$. When the incident angle $\theta_i < \theta_c$, there will be anomalous refraction. When $\theta_i > \theta_c$, k_{2y}^t will be imaginary and the incident wave will be totally reflected. If $\varepsilon_{rz}\mu_{ry} \geq \varepsilon_{r1}\mu_{r1}$, the critical angle $\theta_c = \pi/2$. In this case, for any incident angles, there will be anomalous refraction.

CASE2. $\mu_y < 0$, $\mu_x > 0$, $\varepsilon_z > 0$

From Eq. (7), the components of the wave vector $\boldsymbol{k}_2^t$ in the wave-vector surface satisfy a two-sheeted hyperboloid expression $-k_x^2/|\mu_y\varepsilon_z| + \left(k_{2y}^t\right)^2/(\varepsilon_z\mu_x) = \omega^2$. In this case, the inequality (11) is always right and there will be anomalous refraction for any incident angles.

CASE3. $\mu_y < 0$, $\mu_x > 0$, $\varepsilon_z < 0$

From Eq. (7), the components of the wave vector $\boldsymbol{k}_2^t$ in the wave-vector surface satisfy a one-sheeted hyperboloid expression $k_x^2/(\mu_y\varepsilon_z) - \left(k_{2y}^t\right)^2/|\varepsilon_z\mu_x| = \omega^2$. From Eq. (11), there also exists a critical angle $\theta_c = \arcsin\sqrt{(\varepsilon_z\mu_y)/(\varepsilon_1\mu_1)} = \arcsin\sqrt{(\varepsilon_{rz}\mu_{ry})/(\varepsilon_{r1}\mu_{r1})}$. However, the occurrence of anomalous refraction will require that the incident angle must be larger than this critical angle, namely $\theta_i > \theta_c$. If the incident angle is smaller than the critical angle, namely $\theta_i < \theta_c$, k_{2y}^t will be imaginary and the incident wave will be totally reflected. If $\varepsilon_{rz}\mu_{ry} \geq \varepsilon_{r1}\mu_{r1}$, the critical angle $\theta_c = \pi/2$. In this case, for any incident angles, the incident wave will be totally reflected.

After the anomalous refraction takes place, let us determine the refraction angle. From Eq. (5),we can find that some separation angle exists between the wave vector $\boldsymbol{k}_2^t$ and the Poynting vector $\boldsymbol{S}_2^t$. So there will be two refraction angles in Region 2 for a given incident angle θ_i, one is the refraction angle of the wave vector θ_k, the other is that of the Poynting vector θ_s. θ_k can be simply obtained by the dispersion relation (7) and the matching condition $k_1^i \sin\theta_i = k_2^t \sin\theta_k$, while θ_s can obtained by computing the gradient of the dispersion relation [18]. After some simple algebra, the generalization of Snell's law reads

$$\sin\theta_k = \frac{\sin\theta_i}{\sqrt{\dfrac{\varepsilon_z\mu_x}{\varepsilon_1\mu_1} + \left(1 - \dfrac{\mu_x}{\mu_y}\right)\sin^2\theta_i}} = \frac{\sin\theta_i}{\sqrt{\dfrac{\varepsilon_{rz}\mu_{rx}}{\varepsilon_{r1}\mu_{r1}} + \left(1 - \dfrac{\mu_{rx}}{\mu_{ry}}\right)\sin^2\theta_i}} \tag{14}$$

$$\sin\theta_s = \frac{\sin\theta_i}{\sqrt{\dfrac{\varepsilon_z\mu_y}{\varepsilon_1\mu_1} - \left(1 - \dfrac{\mu_x}{\mu_y}\right)\sin^2\theta_i}}\sqrt{\frac{\mu_x}{\mu_y}}$$
$$= \frac{\sin\theta_i}{\sqrt{\dfrac{\varepsilon_{rz}\mu_{ry}}{\varepsilon_{r1}\mu_{r1}} - \left(1 - \dfrac{\mu_{rx}}{\mu_{ry}}\right)\sin^2\theta_i}}\sqrt{\frac{\mu_{rx}}{\mu_{ry}}} \tag{15}$$

In this paper, we define all angles with respect to the $+y$ axis in a range of $(-\pi, \pi)$. From Fig. 1, the range of the angle is $(-\pi, 0)$ at $x < 0$ and $(0, \pi)$ at $x > 0$. So the incident angle θ_i belongs to $(0, \pi/2)$. Because the power of the refracted wave locates on the left side of the $+y$ axis and flows away from the interface upward, so the refraction angle of the Poynting vector θ_s belongs to $(-\pi/2, 0)$ and it can be obtained by the transformation $\theta_s \to -\theta_s$ after the calculation from Eq. (15) for a given incident angle θ_i. As to that of the wave vector θ_k, if the y component of the wave vector k_{2y}^t is larger than zero and it can be obtained by directly calculated from Eq. (14), if k_{2y}^t is less than zero and it can be obtained by the transformation $\theta_k \to \pi - \theta_k$ after the calculation from Eq. (14).

4. NUMERICAL RESULTS

In this section, the FDTD method based on the Drude dispersive models is employed to study the anomalous refraction or reflection of the CW TE-polarized Gaussian Beam (E_z, H_x, H_y) passing from free space into BA-LHMs with several sets of constitutive parameters. The principal components of the tensors in Eq. (1) can be expressed by the Drude dispersive models as follows

$$\varepsilon(\omega) = \varepsilon_0\left[1 - \frac{\omega_{pe}^2}{\omega\left(\omega - i\Gamma_e\right)}\right], \quad \mu(\omega) = \mu_0\left[1 - \frac{\omega_{pm}^2}{\omega\left(\omega - i\Gamma_m\right)}\right] \tag{16}$$

where ω_{pe}, ω_{pm} are the plasma frequencies and Γ_e, Γ_m are the collision frequencies of the electric and magnetic properties, respectively and negative permittivity and permeability components can be realized by changing them.

In the following simulations, Region 1 stands for free space with $\varepsilon_1 = \varepsilon_0$, $\mu_1 = \mu_0$, $k_1^i = k_1^r = k_0$ and Region 2 stands for BA-LHMs with ε_z, μ_x, μ_y. The x-y FDTD space is 800×400 cells with a four-cell-layer PML absorbing boundary [19]. The cell sizes are

$\Delta x = \Delta y = \lambda_0/20 = 0.05\,\text{cm}$, corresponding to $f_0 = 30\,\text{GHz}$. The time step is chosen as $\Delta t = 0.95\Delta x/\left(\sqrt{2}c_0\right) = 1.1195\,\text{ps}$. And the waist of the Gaussian Beam is $W_0 = 100\Delta x = 5\,\text{cm}$.

4.1. $\mu_y < 0$, $\mu_x < 0$, $\varepsilon_z < 0$

CASE1: $\mu_y = -\left(\sqrt{2}/2\right)\mu_0$, $\mu_x = -\mu_0$, $\varepsilon_z = -\left(\sqrt{2}/2\right)\varepsilon_0$

Choose $\omega_{pmy} = \omega_{pez} = 2\pi\sqrt{\left(1+\sqrt{2}/2\right)}f_0$, $\omega_{pmx} = 2\pi\sqrt{2}f_0$ and $\Gamma_e = \Gamma_m = 0$ in Eq. (16), then the parameters above can be obtained and the critical angle is $\theta_c = \arcsin\left(\sqrt{2}/2\right) = \pi/4$. In this case, the components of the wave vector $\boldsymbol{k}_2^t$ in the wave-vector surface satisfy $2k_x^2 + \sqrt{2}\left(k_{2y}^t\right)^2 = k_0^2$ and those of the wave vector in Region 1 satisfy $k_x^2 + k_y^2 = k_0^2$, as shown in Fig. 2(a).

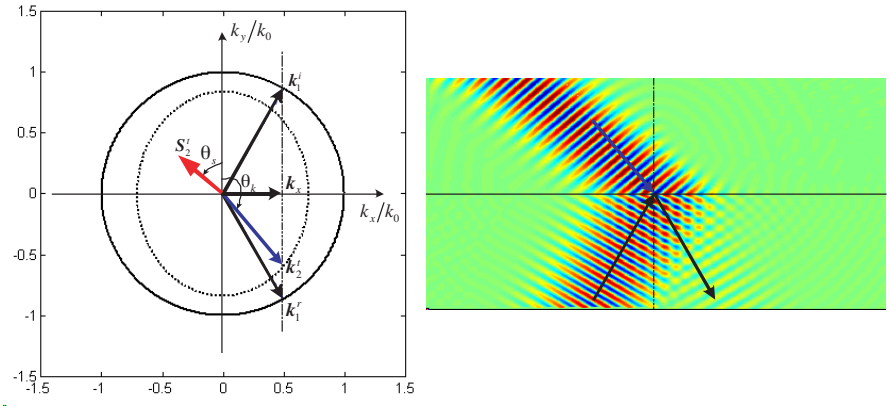

(a) (b)

Figure 2. Simulation results when incident angle $\theta_i = \pi/6$, (a) diagram for wave-vector surface, (b) electric fields distributions.

Firstly, the incident angle $\theta_i = \pi/6$ is employed. From Fig. 2(a), k_{2y}^t may have two values at the matching $k_{2x}^t = k_x > 0$. For $\mu_x < 0$, so $k_{2y}^t < 0$ can be obtained from Eq. (12), and then $\boldsymbol{k}_2^t = k_x\boldsymbol{e}_x - \left|k_{2y}^t\right|\boldsymbol{e}_y$. From Eqs. (14) and (15), we can obtain two refraction angles: $\theta_k = 0.7774\pi$ and $\theta_s = -0.2774\pi$, as the blue and red arrows respectively shown in Fig. 2(a). Note that the red arrow in Fig. 2(a) only stands for the direction of the Poynting vector of the refracted wave, not its

value. Fig. 2(b) presents the electric fields distributions in the whole simulation space. Time animations illustrate that the phase front of the Gaussian Beam in Region 2 does progresses downward to the interface in the direction of the blue arrow and the power flows away from the interface in the direction of the red arrow. That the incident and refracted waves are both on the same side of the normal shows the anomalous refraction has taken place when $\theta_i < \theta_c$.

Secondly, the incident angle $\theta_i = (11\pi)/36$ is employed. From Fig. 3(a), k_{2y}^t must be imaginary at the matching $k_{2x}^t = k_x$. From the analysis above, the electric field of the refracted wave $\boldsymbol{E}_2^t$ will attenuate exponentially in the y direction and the incident wave will be totally reflected. Fig. 3(b) presents the electric fields distributions in the whole simulation space. The penetrating electric field in Region 2 is too weak and does attenuate exponentially in the $y$direction. And the incident wave in Region 1 is indeed totally reflected when $\theta_i > \theta_c$.

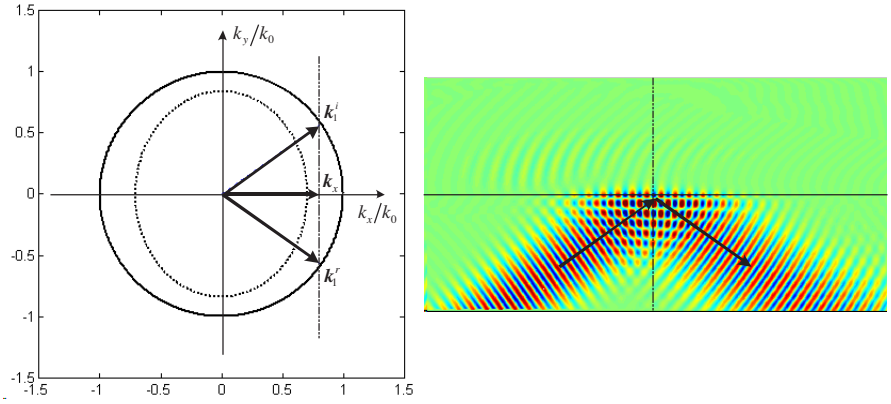

(a) (b)

Figure 3. Simulation results when incident angle $\theta_i = 11\pi/36$, (a) diagram for wave-vector surface, (b) electric fields distributions.

CASE2: $\mu_y = -\mu_0$, $\mu_x = -\mu_0$, $\varepsilon_z = -\varepsilon_0$

Choose $\omega_{pmy} = \omega_{pmx} = \omega_{pez} = 2\pi\sqrt{2}f_0$ and $\Gamma_e = \Gamma_m = 0$ in Eq. (16), then the parameters above can be obtained and the critical angle is $\theta_c = \pi/2$. In this case, the materials in Region 2 are just isotropic LHMs. The components of the wave vector in Region 1 and 2 both satisfy $k_x^2 + k_y^2 = k_0^2$ in the wave-vector surface, as shown in Fig. 4(a). From the analysis above, there will be anomalous refraction for any incident angles.

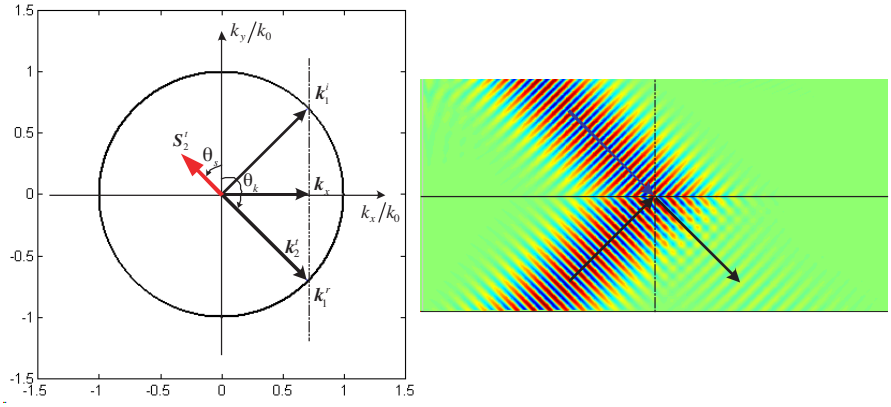

(a) (b)

Figure 4. Simulation results when incident angle $\theta_i = \pi/4$, (a) diagram for wave-vector surface, (b) electric fields distributions.

Here the incident angle $\theta_i = \pi/4$ is employed, From Eqs. (14) and (15), we can obtain two refraction angles: $\theta_k = 3\pi/4$ and $\theta_s = -\pi/4$, as the blue and red arrows respectively shown in Fig. 4(a). Fig. 4(b) presents the electric fields distributions in the whole simulation space. Time animations illustrate that the Poynting vector $\boldsymbol{S}_2^t$ and the wave vector $\boldsymbol{k}_2^t$ are antiparallel in Region 2 and the anomalous refraction has taken place for any incident angles.

4.2. $\mu_y < 0$, $\mu_x > 0$, $\varepsilon_z > 0$

Choose $\omega_{pmy} = 2\pi\sqrt{2}f_0$, $\omega_{pmx} = \omega_{pez} = 0$ and $\Gamma_e = \Gamma_m = 0$ in Eq. (16), then the parameters $\mu_y = -\mu_0$, $\mu_x = +\mu_0$ and $\varepsilon_z = +\varepsilon_0$, can be obtained. In this case, the components of the wave vector $\boldsymbol{k}_2^t$ in the wave-vector surface satisfy $-k_x^2 + \left(k_{2y}^t\right)^2 = k_0^2$, as shown in Fig. 5(a). For any incident angles, the inequality (11) is always right and k_{2y}^t is always real, so there will be anomalous refraction no matter what incident angles are.

In this case, the incident angle $\theta_i = \pi/4$ is employed. From Fig. 5(a), for $\mu_x > 0$, so $k_{2y}^t > 0$ can be obtained from Eq. (12), and then $\boldsymbol{k}_2^t = k_x\boldsymbol{e}_x + \left|k_{2y}^t\right|\boldsymbol{e}_y$. From Eqs. (14) and (15), we can obtain two refraction angles: $\theta_k = \pi/6$ and $\theta_s = -\pi/6$, as the blue and red arrows respectively shown in Fig. 5(a). Fig. 5(b) presents the electric fields distributions in the whole simulation space. Time animations

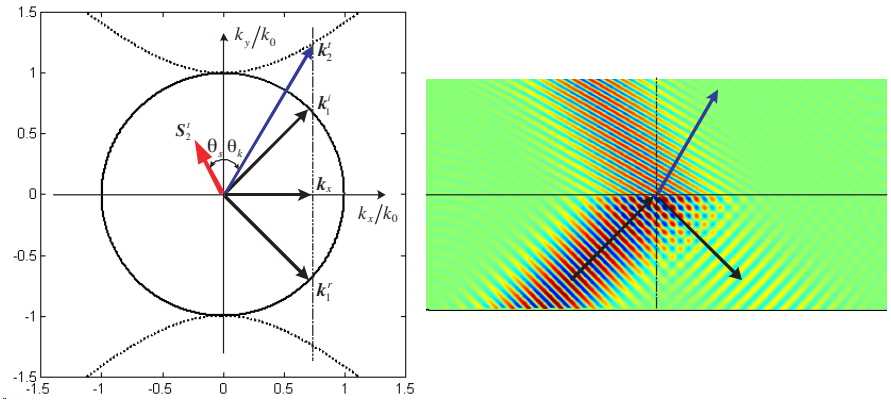

(a) (b)

Figure 5. Simulation results when incident angle $\theta_i = \pi/4$, (a) diagram for wave-vector surface, (b) electric fields distributions.

illustrate that the phase front of the Gaussian beam in Region 2 does progresses in the direction of the blue arrow and the power flows away from the interface in the direction of the red arrow, which proves that there is anomalous refraction for any incident angles.

4.3. $\mu_y < 0$, $\mu_x > 0$, $\varepsilon_z < 0$

CASE1: $\mu_y = -\left(\sqrt{2}/2\right)\mu_0$, $\mu_x = +\mu_0$, $\varepsilon_z = -\left(\sqrt{2}/2\right)\varepsilon_0$

Choose $\omega_{pmy} = \omega_{pez} = 2\pi\sqrt{\left(1+\sqrt{2}/2\right)}f_0$, $\omega_{pmx} = 0$ and $\Gamma_e = \Gamma_m = 0$ in Eq. (16), then the parameters above can be obtained and the critical angle is $\theta_c = \arcsin\left(\sqrt{2}/2\right) = \pi/4$. In this case, the components of the wave vector $\boldsymbol{k}_2^t$ in the wave-vector surface satisfy $2k_x^2 - \sqrt{2}\left(k_{2y}^t\right)^2 = k_0^2$ and those of the wave vector in Region 1 satisfy $k_x^2 + k_y^2 = k_0^2$, as shown in Fig. 6(a).

Firstly, the incident $\theta_i = \pi/6$ is employed. From Fig. 6(a), k_{2y}^t must be imaginary at the matching $k_{2x}^t = k_x$. From the analysis above, the incident waves will be totally reflected. Fig. 6(b) presents the electric fields distributions in the whole simulation space. The incident wave in Region 1 is indeed totally reflected only when $\theta_i < \theta_c$.

Secondly, the incident angle $\theta_i = (13\pi)/36$ is employed. From Fig. 7(a), for $\mu_x > 0$, so $k_{2y}^t > 0$ can be obtained from Eq. (12), and

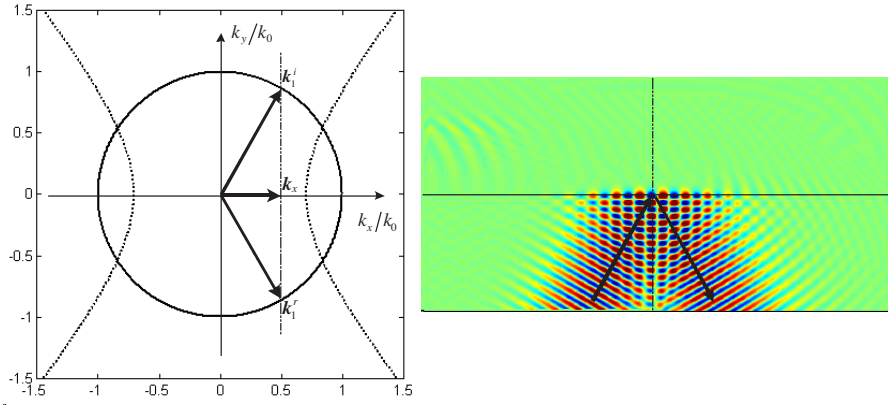

(a) (b)

Figure 6. Simulation results when incident angle $\theta_i = \pi/6$, (a) diagram for wave-vector surface, (b) electric fields distributions.

then $\boldsymbol{k}_2^t = k_x \boldsymbol{e}_x + \left|k_{2y}^t\right| \boldsymbol{e}_y$. From Eqs. (14) and (15), we can obtain two refraction angles: $\theta_k = 0.2964\pi$ and $\theta_s = -0.3459\pi$, as the blue and red arrows respectively shown in Fig. 7(a). Fig. 7(b) presents the electric fields distributions in the whole simulation space. Time animations illustrate that there is anomalous refraction when the incident angle is larger than the critical angle, namely $\theta_i > \theta_c$. However no totally reflection takes place in this case, which is significantly different from that in isotropic LHMs.

CASE2: $\mu_y = -\mu_0$, $\mu_x = +\mu_0$, $\varepsilon_z = -\varepsilon_0$

Choose $\omega_{pmy} = \omega_{pez} = 2\pi\sqrt{2}f_0$, $\omega_{pmx} = 0$ and $\Gamma_e = \Gamma_m = 0$ in Eq. (16), then the parameters above can be obtained and the critical angle is $\theta_c = \pi/2$. In this case, the components of the wave vector $\boldsymbol{k}_2^t$ in the wave-vector surface satisfy $k_x^2 - \left(k_{2y}^t\right)^2 = k_0^2$, as shown in Fig. 8(a). From the analysis above, the incident wave will be totally reflected for any incident angles. Here the incident angle $\theta_i = \pi/4$ is employed, Fig. 8(b) presents the electric fields distributions in the whole simulation space. The incident wave is indeed totally reflected, which validates the theoretical analysis.

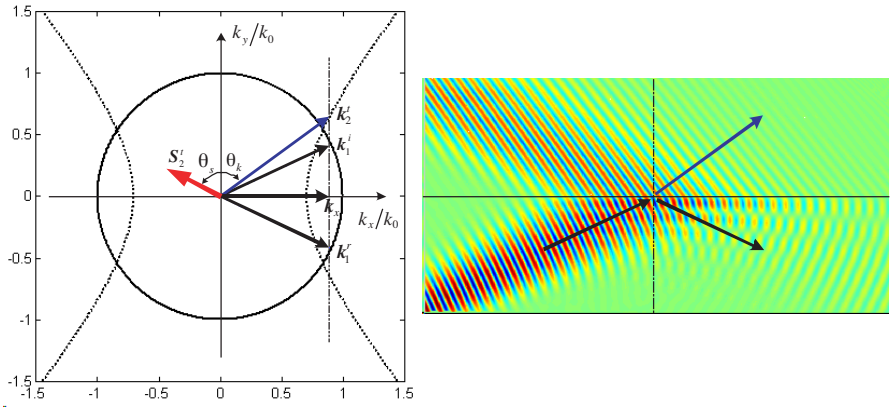

(a) (b)

Figure 7. Simulation results when incident angle $\theta_i = 13\pi/36$, (a) diagram for wave-vector surface, (b) electric fields distributions.

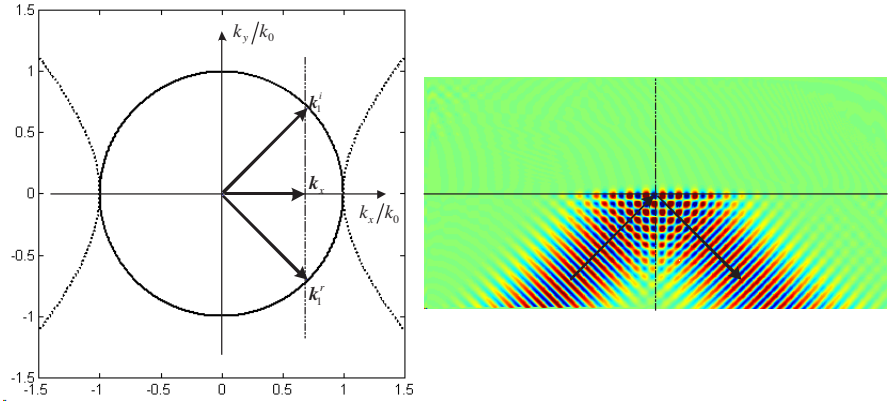

(a) (b)

Figure 8. Simulation results when incident angle $\theta_i = \pi/4$, (a) diagram for wave-vector surface, (b) electric fields distributions.

5. CONCLUSION

This paper has presented the investigations on the anomalous characteristics of electromagnetic wave propagation in BA-LHMs theoretically and numerically in detail. The conditions that the anomalous refraction or reflection will occur at the interface when the TE polarized plane wave passes from one isotropic right-handed

material into another BA-LHM have been studied and discussed emphatically. Meanwhile the corresponding numerical results by FDTD based on the Drude dispersive models are presented with different sets of constitutive parameters of BA-LHMs. The simulated results are in agreement with theoretical analysis, which will be helpful for the studies on the electromagnetic characteristics of anisotropic LHMs further.

REFERENCES

1. Veselago, V. G., "The electrodynamics of substances with simultaneously negative values of ε and μ," *Sov. Phys. Usp.*, Vol. 10, 509–515, 1968.
2. Pendry, J. P., A. J. Holden, D. J. Robbins, and W. J. Stewart, "Low frequency plasmons in thin-wire structures," *J. Phys. Condens. Matter.*, Vol. 10, 4785–4809, 1998.
3. Pendry, J. P., A. J. Holden, D. J. Robbins, and W. J. Stewart, "Magnetism from conductors and enhanced nonlinear phenomena," *IEEE Trans. Microwave Theory Tech.*, Vol. 47, 2075–2084, 1999.
4. Smith, D. R., W. J. Padilla, D. C. Vier, S. C. Nemat-Nassser, and S. Schultz, "Composite medium with simultaneously negative permeability and permittivity," *Phys. Rev. Lett.*, Vol. 84, 4184–4187, 2000.
5. Shelby, R. A., D. R. Smith, and S. Schultz, "Experimental verification of a negative index of refraction," *Science*, Vol. 292, 77–79, 2001.
6. Lindell, I. V., S. A. Tretyakov, K. I. Nikoskinen, and S. Ilvonen, "BW media-media with negative parameters, capable of supporting backward waves," *Microwave Opt. Technol. Lett.*, Vol. 31, 129–133, 2001.
7. Hu, L. B. and S. T. Chui, "Characteristics of electromagnetic wave propagation in uniaxially anisotropic left-handed materials," *Phys. Rev. B*, Vol. 66, 085108:1–7, 2002.
8. Hu, L. B and Z. F. Lin, "Imaging properties of uniaxially anisotropic negative refractive index materials," *Phys. Rev. Lett. A*, Vol. 313, 316–324, 2003.
9. Karkkainen, M. K., "Numerical study of wave propagation in uniaxially anisotropic Lorentzian backward-wave slabs," *Phys. Rev. E*, Vol. 68, 026602:1–6, 2003.
10. Geng, Y. L. and S. L. He, "Analytical solution for electromagnetic

scattering from a sphere of uniaxial left-handed material," *J. Zhejiang Univ. Science A*, Vol. 7, 99–104, 2006.

11. Ziolkowski, R. W. and E. Heyman, "Wave propagation in media having negative permittivity and permeability," *Phys. Rev. E*, Vol. 64, 056625, 2001.
12. Ziolkowski, R. W., "Pulsed and CW Gaussian beam interactions with double negative metamaterial slabs," *Opt. Express*, Vol. 11, 662–681, 2003.
13. Huangfu, J., L. Ran, H. Chen, X. Zhang, K. Chen, T. M. Grzegorczyk, and J. A. Kong, "Experimental confirmation of negative refractive index of a metamaterial composed of Ω-like metallic patterns," *Appl. Phys. Lett.*, Vol. 84, 1537–1539, 2004.
14. Chen, H., L. Ran, J. Huangfu, X. Zhang, K. Chen, T. M. Grzegorczyk, and J. A. Kong, "Left-handed metamaterials composed of only S-shaped resonators," *Phys. Rev. E*, Vol. 70, 057605, 2004.
15. Chen, H., L. Ran, J. Huangfu, X. M. Zhang, K. Chen, T. M. Grzegorczyk, and J. A. Kong, "Magnetic properties of S-shaped split-ring resonators," *Progress In Electromagnetics Research*, PIER 51, 231, 2005.
16. Ran, L., J. Huangfu, H. Chen, X. M. Zhang, K. Chen, T. M. Grzegorczyk, and J. A. Kong, "Experimental study on several left-handed matamaterials," *Progress In Electromagnetics Research*, PIER 51, 249, 2005.
17. Smith, D. R. and D. Schurig, "Electromagnetic wave propagation in media with indefinite permittivity and permeability tensors," *Phys. Rev. Lett.*, Vol. 90, 077405, 2003.
18. Kong, J. A., *Electromagnetic Wave Theory*, EMW, New York, 2000.
19. Cummer, S. A., "Perfectly matched layer behavior in negative refractive index materials," *IEEE Antennas and Wireless Propagation Letters*, Vol. 3, 2004.